CHAPTER VII
IN-SITU HYBRID COMPOSITES OF POLY(ETHYLENE TEREPHTHALATE)/ LIQUID CRYSTALLINE POLYMER FILLED WITH MICROWAVE-SYNTHESIZED ZINC OXIDE POWDER

7.1 Abstract

Blends of Poly(ethylene terephthalate) (PET) with 10 wt% liquid crystalline polymer (LCP) were filled with zinc oxide powder (ZnO) at 0.5 and 1.0 phr loadings. The ZnO powder was synthesized via microwave irradiation in an aqueous system. Melt-blending was conducted in a twin-screw extruder and the obtained compounds were then injection-molded. It was hypothesized that the transesterification between the LCP and PET might be promoted by the catalytic activity of ZnO, yielding a composite with better mechanical performance. A reduction in an LCP fibril fraction in PET matrix, along with a lower shear viscosity, was observed with increasing ZnO loading. The LCP was found to enhance both isothermal and non-isothermal crystallization kinetics of PET, whereas ZnO retarded them. The tensile strength upon the addition of ZnO indicated no improvement of the interface adhesion between LCP and PET such that the significant occurrence of a transesterfication was unlikely. ZnO was found to increase the tensile modulus of the PET/LCP blends.

Key words: In-Situ Composites; Liquid Crystalline Polymer; Microwave; Zinc Oxide

7.2 Introduction

It is widely accepted that the use of short glass fibers as a reinforcing agent can considerably improve the mechanical strength and stiffness of polymers. However, conventional polymer composites usually require a high load of glass fibers making

them more difficult to process because of the rise in melt viscosity. Other difficulties encountered include wear of processing facility caused by the abrasion of reinforcement and fiber breakage. To overcome these problems, blending of a thermoplastic with a highly rigid, non-abrasive component yet not hinder the polymer flow would be fascinating. The potential candidate as a substitute for glass fibers is the liquid crystalline polymer (LCP). Under optimized flow conditions, the LCP can align themselves and elongate to the direction of flow, resulting in a reduction in melt viscosity and improved mechanical properties. Thus the LCP/TP blends are usually termed 'in-situ composites'. Blending of an LCP with a thermoplastic also help reduce the cost as an LCP alone is too expensive to be used in domestic and some engineering applications.

There are many studies dealing with systems containing an LCP and various inorganic solid reinforcements, such as glass fiber [1,2], carbon black [3,4], whisker [5,6] and silica [7,8]. The final properties of the systems depend critically not only on the blend morphology but also on the interfacial properties between the thermoplastic matrix and the reinforcing LCP domains. To attain the improved mechanical performance, sometimes calls for the additional enhancement of interfacial adhesion, probably by the use of the polymeric compatibilizing agents. A compatibilizing agent may be added to the blend as a third component or may be generated during reactive mixing of the blend. The latter (also referred to as in situ compatibilization) may involve transesterification provided that the system contains ester exchange reactive groups. The resulting copolymers will be located at the polymer interfaces providing lower interfacial tension and better adhesion which lead to effective stress transfer at the interface. An example of such an approach was demonstrated by blending polycarbonate with Vectra A950, both of which contain ester linkages that can be inter-exchangeable. Tovar *et al.* [9] observed better dispersion as well as mechanical properties of PC/VA 950 at a greater tranesterification extent. The exchange reactions were also observed between Vectra B950 and PET [10]. In some cases, adding a nano-sized inorganic filler can improve compatibility of the blends such as nano-clay [11] in Polyamide6/LCP blends, carbon nanotube in PC/LCP blends [12]. Nonetheless, up to now there has been no

research that utilizes metal oxides in the system of in-situ composites. Among the metal oxides, zinc oxide (ZnO) is an inorganic material that has been widely used as an additive in numerous materials including plastics, ceramics, glass, cement, rubber, lubricants, paints, adhesives, pigments, retardants, etc. Polymer composites of various forms of ZnO were obtained with improved properties, i.e. the use of ZnO of pigmentary grade (150-200 nm mean particle size) can give protection in UV absorbing acrylic composites [13]. The nano-sized ZnO particles (53 nm) have been reported to increase hardness and reduce the wear rate with respect to the neat PC [14]. Also, ZnO coatings can protect PC films against UV radiation [15]. It has been known that the alteration of the resulting composite properties depends on the type of matrix polymer and the characteristics of the ZnO used (size, distribution, dispersion, surface properties) together with the interfacial adhesion [14]. Recently, S. Wacharawichanant investigated the polyoxymethylene (POM)/ZnO composites with different ZnO particle sizes. They found that the smaller ZnO particles rendered composites with better mechanical properties than the larger ZnO particles do. However, the latter shows better ZnO dispersion at high ZnO loadings [16]. Coltelli et. al. [17] compared ZnO and a stronger nucleophilic zinc derivative, the zinc acetate ($ZnAc_2$) on their catalytic reactivity for a tranesterfication reaction between dibutyl maleate functionalized poly(ethylene) (POF) and PET. The nucleophilic character of the zinc derivatives plays the key role to PET degradation; i.e. the stronger the catalyst nucleoplilicity, the greater the tendency for PET to undergo nucleophilic substitution with the catalysts, leading to its degradation. Based on this criterion, ZnO was expected to contribute to much less PET degradation compared to $ZnAc_2$. The same authors reported that ZnO was able to produce a certain amount of PET-POF copolymer without leading to PET degradation.

In this contribution, we prepared the composites of PET/LCP with well-dispersed ZnO particles. ZnO particles were synthesized by water-based, microwave radiation – a green synthesis method. The rheological, morphological, thermal and mechanical properties will be discussed.

7.3 Experimental

7.3.1 Materials

Poly(ethylene terephthalate) (PET) was RAMAPET N1, purchased from Indorama Polymers Public Company Limited, Thailand. The LCP used was Vectra A950 (labeled VA hereafter), kindly supplied by Hoechst-Celanese. VA is a copolyester of 73 mol% p-hydroxybenzoic acid (HBA) and 27 mol% 2-hydroxy-6-naphthoic acid (HNA). All the materials were dried in a vacuum oven at 120°C for at least 12 h prior to use.

7.3.2 Microwave-Assisted Synthesis of ZnO Powder

$Zn(NO_3)_2 \cdot 6H_2O$ (99.5 mol%, Carlo Erba) and solid NaOH (Labscan) were seperately dissolved in 50 ml of deionized water and stirred using a magnetic stirrer for 30 min at room temperature. Then the two solutions were mixed together with an additional 100 ml of deionized water to yield a final 200 ml solution. The solution was then immediately irradiated by a microwave in a domestic microwave oven (Samsung, M-183GN, 2.45 GHz, 850W) in air for 5 min. The products were separated by centrifugation, then washed with deionized water three times, and dried at 70°C under atmospheric pressure. The ZnO nanoparticles were characterized by XRD and SEM.

7.3.3 Preparation of Blends

PET, VA resins and ZnO powder were premixed in a dry mixer to prepare PET/VA blends with a VA content of 10 wt% and ZnO of 0, 0.5, and 1.0 phr with respect to the total polymer weight. The compounds were designated as shown in Table 7.1. The dry-mixed blends were melt-mixed in a self-wiping, co-rotating twin-screw extruder (Collin, ZX-25). The temperature of the barrel section from the feeding zone to the die was set at 95, 250, 260, 270, 275, 265°C. The rotor was operated at a speed of 20 rpm. The extrudates were cooled by water and then pelletized.

The neat PET and the blends, with or without ZnO, were injected into dumbbell-shaped specimens 2.5 mm thick on an AP-90 (Asian Plastic) injection molding machine for the tensile tests. The injection molding conditions are provided in Table 7.2.

7.3.4 Rheological Measurement

The shear viscosity of the blends was measured using a CEAST Rheologic 5000 twin-bore capillary rheometer with the inner diameter and the length of the barrel of 15 and 250 mm, respectively, and the inner diameter and the length of the die were 1 and 20 mm (i.e. L/D ratio = 20), respectively. The temperature tolerance was set at ±0.5°C. The measurement was done 260°C and a shear rate range of 200–6,400 s^{-1}. The rheometer extrudates were quenched at room temperature and collected for further SEM analysis.

7.3.5 Morphological Observation

The morphological study was conducted using a JEOL JSM5200 scanning electron microscope (SEM). The specimens were cryogenically fractured in liquid nitrogen to provide a cross-sectional view. The rheometer extrudates were also immersed in 2-chlorophenol at 80°C for 2 h to dissolve the PET matrix as the first step, followed by repeated washing of the VA residue. The fractured surfaces and the VA residue were sputtered with a thin layer of gold prior to observation. Energy dispersive X-ray (EDX) analysis was also performed to evaluate the dispersion of the Zn element in the composites.

7.3.6 DSC Characterization

The differential scanning calorimeter measurements were carried out using a Perkin-Elmer DSC7 differential scanning calorimeter (DSC). All measurements were performed under a dry nitrogen atmosphere at a flow rate of 20 ml/min. The standard sample used was indium. Each sample holder was loaded with samples of comparable quantity (7±0.5 mg). All the experiments started with heating the sample

from 25°C to a fusion temperature of 310°C at a heating rate of 200°C min^{-1} for a melt-annealing period of 5 min in order to remove previous thermal histories, after which the samples were cooled at a rate of 10°C/min to 25°C. The sample was then heated to 300°C at a heating rate of 10°C min^{-1}. For the study of the isothermal crystallization behavior, after the melt-annealing, the sample was cooled from 310°C to the predetermined crystallization temperature of 200°C and maintained until the crystallization of the PET matrix was complete.

7.3.7 Investigation on Mechanical Performance

To measure the mechanical properties of the samples, tensile testing results were averaged from at least five samples using an Instron 4206 tensile tester at room temperature with an extension speed of 5 mm/min and an initial gauge length of 25 mm. The mechanical properties (tensile modulus, tensile strength, and percent elongation at break) were determined from the stress–strain curve.

7.4 Results and Discussion

7.4.1 Characterization of ZnO Powder

Fig. 7.1 displays the X-ray diffraction patterns of the obtained powders, corresponding to the hexagonal wurtzite structure of ZnO. The sharp diffraction peaks indicated high crystallinity of the synthesized ZnO powder. Using the Debye-Scherrer formula as shown in Eq. (7.1), the crystallite size (D) was found to be approximately 26.6 nm.

$$D = \frac{0.9\lambda}{B\cos\theta_B} \qquad (7.1)$$

From the SEM image shown in Fig. 7.2, the synthesized ZnO powder consisted of fairly uniform spherical particles with an agglomerate size of 170±0.03 nm. Each ZnO agglomerate was therefore the combination of 6-7 crystallites.

7.4.2 Rheological Results

Fig.7.3. displays the viscosity data as a function of shear rate for the pure polymers (PET and VA), the neat blends (PET/VA) and the composites (PET/VA/ZnO). VA shows the strongest non-Newtonion behavior implying that the VA molecules can most readily be oriented under the shear flow. The shear viscosity of the neat VA is the greatest at shear rate up to 1000 s^{-1}, and then becomes comparable to that of PC. The PET/VA blend shows a viscosity reduction as compared to the pristine PET. Such reduction originates from the chain alignment of VA and partly to the interfacial slip between the LCP and the matrix. Further viscosity reduction is found with increasing ZnO loading. One may think of a viscosity reduction as an indicator of a decreased molecular weight as a consequence of polymeric decomposition. Actually, the zinc derivatives such as zinc acetate, zinc chloride and zinc oxide can serve as a transesterification catalyst. In the chemical recycling of PET, the small molecule ester exchange reagent such as methanol is introduced into the system at elevated pressure and temperature to recover the acid and alcohol components, where the catalyst used may be ZnO [18]. In our experiment, the only ester exchange reactive agents are PET and VA, and consequently it is expected that the most likely chemical reaction to occur would be the transesterification between reactive end-groups of these two polymers. Also, as supported by Coltelli *et al.* [17], the degradation of PET induced by ZnO is negligible. The viscosity reduction is therefore ascribed to the lubricating effect as the spherical ZnO particles may glide the polymeric chain and facilitate the flow of the molten polymer.

7.4.3 SEM Analysis

Fig. 7.4 shows the SEM images of the VA residue taken from injection-molded samples. Both short microfibrils and droplets are obtained in the PET/VA blend. Only the sufficiently large VA domains can undergo deformation during injection-molded according to the definition of the capillary number. Therefore, the observed droplets came from a fraction of VA domains obtained in a twin-screw extruder that

were too small to fibrillate in an injection molding machine and thus retained their spherical shape. The addition of 0.5 phr ZnO, however, results in a loss of fibril fraction. At 1 phr ZnO loading, none of VA fibrils can be found. The EDX element map showing the distribution of zinc is constructed from the fractured surface of PVA 1 ZnO [Fig.7.5]. Good distribution is observed on the PET matrix and the VA domains. Another EDX map in Figs. 7.5 and 7.6 displays the distribution of Zn on the VA residue, reassuring the existence of Zn adhering on VA domains despite of the removal of PET matrix and the vigorous washing of the VA residue.

7.4.4 DSC Analysis

As displayed in Fig. 7.7, the neat PET shows single melting peak belonging to the PET phase whereas those of the blends either with or without ZnO particles exhibit double melting peaks. VA shows a small endothermic peak due to the crystalline-to-nematic transition at around 280°C. From the peak positions, it can be expected that peak I and peak II belong to the crystallization fraction of PET. In other words, PET and VA crystallize separately. The bimodal shape of the melting peaks could be a result of the melting–recrystallization process. According to the literature, the multiple melting phenomenon observed in PET and PET-based composites mostly arises from the melting–recrystallization process of the materials [19,20]. In this case, it is possible that peak I is the first melting of the crystallites formed during a cooling scan while peak II is the melting of the recrystallized materials. However, it is well known that introducing a foreign material into a semi-crystalline polymer can disrupt crystallization process, thus rendering imperfect crystallites. These imperfect crystallites can appear as another melting peak on a lower temperature side [21-23]. Therefore, there are two possibilities that explain the origin of double melting endotherms; the two different crystal qualities or the melting-recrystallization process. To evaluate the origin of double melting endotherms observed in the sample containing VA, the PET/VA blend was crystallized from melt under varied cooling rates ranging from 5 to 30°C/min and then reheated under the same heating rate of 10°C/min. Since the heating rate was kept

constant, its effects on melting-recrystallization behavior (if any), and thermal lag could be eliminated. The heating scans shown in Fig. 7.8 display the double melting endotherms for PET/VA at every cooling rate. Peak I and peak II are assigned to the lower temperature and the higher temperature melting peak, respectively. It is obvious that, contradictory to peak I, peak II becomes more distinct with increasing cooling rate. Generally, a less perfect crystallite melts prior to a more perfect one. If peak I was taken as the melting of a less perfect crystallite population as compared to peak II, the sample crystallized at the lowest cooling rate would have the most perfect crystallites and yield the largest peak II. But the results are found to be the opposite. As a matter of fact, the double melting temperature should have originated from the melting-recrystallization process. Peak I represents the melting of the original crystallites generated during cooling while peak II represents the melting of the recrystallized crystallites. The concave region between the two peaks is then assigned to the recrystallization exotherm. By this assumption, the largest peak II can be found for the sample with the greatest cooling rate, and VA promotes the recrystallization process during the heating scan. Alternately, we also carried out the DSC experiment on the samples where the cooling rate was kept constant (10°C/min) and the heating rate was varied from 5 to 20°C/min. It was found that PET exhibited only monomodal peaks whereas PC/VA showed wholly bimodal peaks (results not shown here) which agrees with our assumption.

Data shown in Table 7.3 are extracted from the thermograms in Fig. 7.9. The initiation temperature of the non-isothermal melt crystallization process (see $T_{mc,on}$) of PET is lower than PVA but higher than those observed from ZnO-containing samples. However, when filled with ZnO, the crystallization process is found to start slightly sooner for a composite with a higher ZnO content. This suggests that VA exhibits a nucleation effect on the PET non-isothermal melt crystallization process. ZnO, on the contrary impedes the PET crystallization probably by impeding polymer chain mobility. A greater ZnO content might lead to a more agglomeration, thus the retardation effect on PET crystallization for the blend with 1 phr ZnO is less pronounced than with 0.5 phr ZnO. Melt crystallization under isothermal conditions is also investigated (see Fig. 7.10).

The crystallization half-time, $t_{1/2}$, defined as the time the polymer takes to reach 50% of its equilibrium crystallinity is the useful parameter to qualitatively compared the crystallization rate. The values of $t_{1/2}$ tabulated in Table 7.4 suggest that the bulk crystallization kinetics are in the following order: PVA > PVA 1 ZnO > PVA 0.5ZnO > PET. The crystallization enthalpy normalized by the weight fraction of PET component (ignoring the weight of ZnO since only a small amount is used) suggests that the degree of crystallinity of PET obtained during the isothermal crystallization is ranked as follows: PVA > PVA 1 ZnO > PVA 0.5 ZnO > PET. It can be concluded that VA has positive effects on PET crystallization, while ZnO has negative effects. Junrong *et al.* [24] studied the role of different sizes of ZnO, from nano- to micrometer-size, on the crystalline structure and crystallization kinetics of nylon-6. They claimed that the ZnO particles induced nylon-6 crystallization from the melt through the nucleation effect. They believed that ZnO could provide ordered surface suitable for the hydrogen bonding formation with nylon-6 and thus facilitate the heterogeneous nucleation process. However, the nucleation effect of ZnO inverses to its size. The crystallization rate is enhanced by this nucleation effect, but can also be retarded by the restriction in polymer chain mobility as a result of polymer-filler interactions. According to the study of crystallization behavior of PET/ZnO nanocomposites done by Junqing *et al.* [25], silane coupling-treated ZnO nanoparticles can accelerate PET crystallization. With the determination of crystallization kinetics via Ozawa model approach [26], they claimed that adding ZnO nanoparticles resulted in an increase in the crystallization growth point. However, it was believed that ZnO in this work did not act as a nucleating agent. This is because the hydrogen bonding formation between the polymer and the filler is not significant in the PET/ZnO system and the ZnO used in this study was unmodified. Another reason may be the lattice mismatch between the hexagonal ZnO and the triclinic PET crystallite [27]. Based on these facts, ZnO would not provide a suitable surface for the PET crystal growth. Instead, the restricted mobility of PET chains by the presence of ZnO retards the crystallization rate. However, introducing VA improves the crystallization process of PET by accelerating the overall crystallization rate of

PC/VA/ZnO along with increasing the normalized degree of crystallinity. Similar observations have been reported Ref. [28, 29] for the blends of PET with an LCP.

7.4.5 Mechanical Performance

The mechanical properties of all samples are reported in Table 7.5. VA provides mechanical reinforcement in the blend as reflected in improved modulus and tensile strength. ZnO promotes only the tensile modulus. The addition of 1 phr ZnO and 10 wt% VA to PET increased the tensile modulus by 29%. The loss of LCP fibrils in the system with ZnO does not have a negative influence on the tensile modulus because the small elongation at which the modulus is measured would prevent filler-matrix debonding. On the other hand, the tensile strength is affected by such loss as this property relies greatly on the interface properties, a key factor that determines the stress transfer. A reduction in the filler aspect ratio leads to a decreased interfacial area necessary for the stress transfer, thus in our system, no improvement in the tensile strength is found. However, the tensile strength of the PET/VA/ZnO composite is retained at a very low ZnO content of 0.5 phr. At 1 phr ZnO loading, the tensile strength was drastically dropped. A decrease in the percent elongation at break is not surprising for the composites filled with either inorganic particles or LCP. Up to this point, the role of ZnO as a catalyst for the transesterification between PET and VA is not evident. The results from tensile properties and the phase morphology imply that there is no improvement in the interfacial properties between PET and VA. Thus, the transesterification products, if existed, are not sufficient to alter the composite properties.

7.5 Conclusions

A liquid crystalline copolyester, Vectra A950 (VA), and a thermoplastic polyester, Poly(ethylene terephthalate) (PET), were melt-blended and filled with small loadings of ZnO particles. It was hypothesized that a tranesterification reaction and a subsequent improvement in interfacial properties might be achieved through a catalytic role of ZnO. Results from the rheology indicated that the apparent shear viscosity decreased by the addition of VA and decreased further with ZnO. The loss of VA microfibrils was ascribed to the lubricating effect of ZnO spherical particles that suppressed the stress PET would have exerted upon VA domains in the absence of ZnO. Molten PET and VA are immiscible and separately crystallized. VA played a nucleating role for PET crystallization while ZnO retarded PET crystallization by restricting PET chain mobility. At a very small ZnO loading of 0.5 phr, the composite was able to retain its tensile strength but this value dropped drastically at a greater ZnO loading, providing an evidence of no enhancement in interfacial adhesion. In other words, the unmodified ZnO used in this study did not promote the tranesterification reaction between PET and VA. The tensile modulus of the composite with 1 phr ZnO increased with a factor of 29%.

7.6 Acknowledgements

Financial support from the Royal Golden Jubilee Ph.D. Program, and The Polymer Processing and Polymer Nanomaterials Research Unit, National Center of Excellence for Petroleum, Petrochemical and Advanced Materials, are gratefully acknowledged.

7.7 References

[1] S. Pisharath, S.C. Wong, Polym. Compos. 24 (2003) 109-118.

[2] H. Liu , K. Liao, J. Appl. Polym. Sci. 94 (2004) 211-221.

[3] K. Dai, X.B. Xu, Z.M. Li, Polymer 48 (2007) 849-859.

[4] K. Dai, Z.M. Li, X.B. Xu, Polymer 49 (2008) 1037-1048.

[5] S.C. Tjong, Y.Z. Meng, Polymer 40 (1999) 1109-1117.

[6] S.C. Tjong, Y.Z. Meng, Polymer 40 (1999) 7275-7283.

[7] J. Chen, P. Chen, L. Wu, J. Zhang, J. He, Polymer 48 (2007) 4242-4251.

[8] M.W. Lee, X. Hu, C.Y. Yue, L. Li, K.C. Tam, Compos. Sci. Technol. 63 (2003) 339-346.

[9] G.Tovar, P. J. Carreau, H. P. Schreiber, Colloids Surf., A 161 (2000) 213-223.

[10] Q. Lin, A.F. Yee, J. Mater. Sci. 32 (1997) 3961-3970.

[11] B. Zhang, Y. Ding,P. Chen, C. Liu, J. Zhang, J. He, G.H. Hue, Polymer 46 (2005) 5385-5395.

[12] M. Mukherjee, T. Das, R. Rajasekar, S. Bose, S. Kumar, C.K. Das, Composites Part A. 40 (2009) 1291-1298.

[13] R.E. Beltrame, M.A. Bos, European Patent EP1697449, 2005.

[14] F.J. Carrión, J. Sanes, M.D. Bermúdez, Wear 262 (2007) 1504-1510.

[15] A. Moustaghfir, E. Tomasella, A. Rivaton, B. Mailhot, M. Jacquet, J. L. Gardette, J. Cellier, Surf. Coat. Technol. 180 (2004) 642-645.

[16] S. Wacharawichanant, S. Thongyai, A. Phutthaphan, C. Eiamsam-ang, Polym. Test. 27 (2008) 971-976.

[17] M.B. Coltelli, M. Aglietto, F. Ciardelli, Eur. Polym. J. 44 (2008) 1512-1524.

[18] F. Ligorati, G. Aglietti, V. E. Nova, U.S. Patent 3776945, 1973.

[19] Y. Lee, R.S. Porter, J.S. Lin, Macromolecules 22 (1989) 1756-1760.

[20] Y.J. Li, X.Y. Zhu, G.H. Tian, D.Y. Yan, E.L. Zhou, Polym. Int. 50 (2001) 677-682.

[21] Y. Wang, J. Deng, K.Wang, Q. Zhang, Q. Fu, J. Appl. Polym. Sci. 104 (2007) 3695-3701.

[22] Y. Kong, J.N. Hay, Polymer 44 (2003) 623-633.

[23] Y. Wang, J. Lu, D.Y. Shen, Polym. J. 32 (2000) 560-566.

[24] J. Zheng, R.W. Siegel, C.G. Toney, J. Polym. Sci., Part B: Polym. Phys. 41 (2003) 1033-1050.

[25] J. He, W. Shao, L. Zhang, C. Deng, C. Li, J. Appl. Polym. Sci. 114 (2009) 1303-1311.

[26] T. Ozawa, Polymer 12 (1971) 150-158.

[27] Z.G. Wang, B.S. Hsiao, B.X. Fu, L. Lui, F. Yeh, B.B. Sauer, H. Chang, J.M. Schultz, Polymer 41 (2000) 1791-1797.

[28] D. Mélot, W. J. MacKnight, Polym. Adv. Technol. 3 (1992) 383-388.

[29] S.H. Kim, S.W. Park, E.S. Gil, J. Appl. Polym. Sci. 67 (1998) 1383-1392.

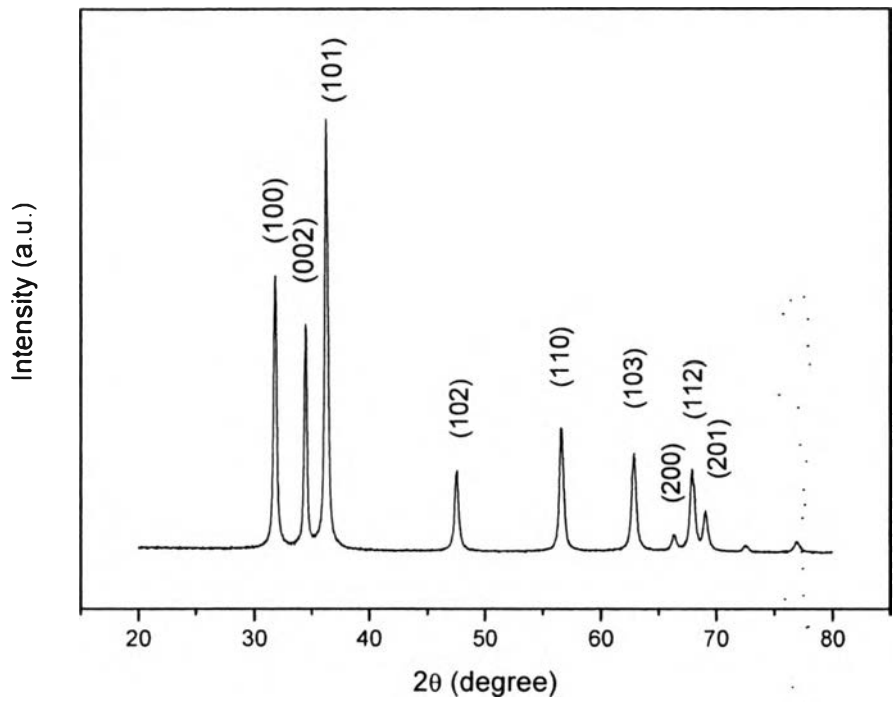

Figure 7.1 XRD spectra of the synthesized ZnO particles.

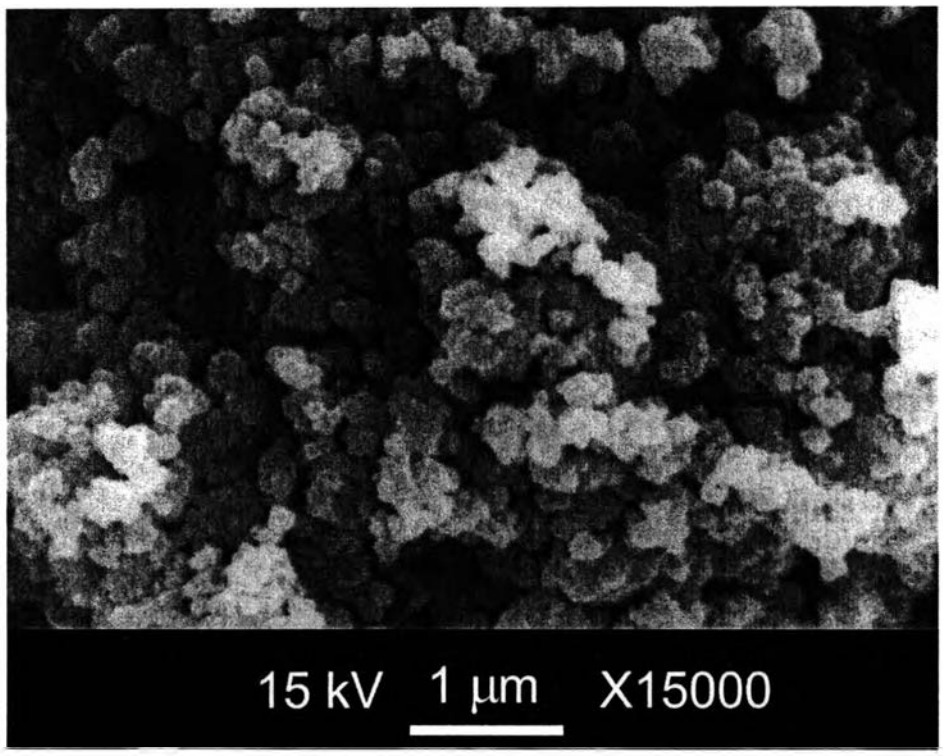

Figure 7.2 SEM image of the synthesized ZnO particles.

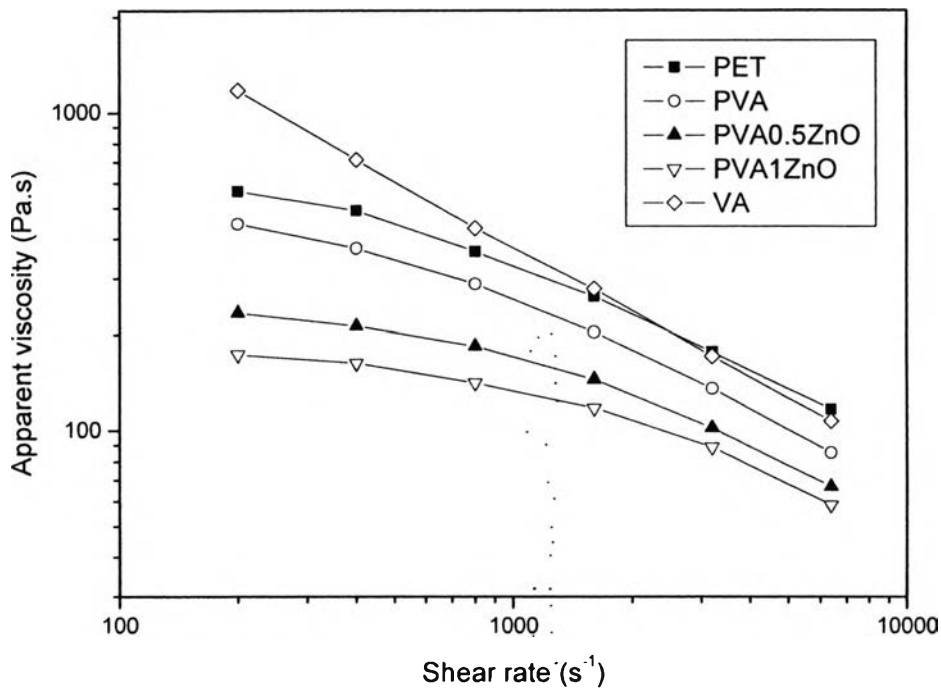

Figure 7.3 Rheological curves of PET, VA, and their blends with ZnO extruded through a capillary die (L/D = 20), at 260°C.

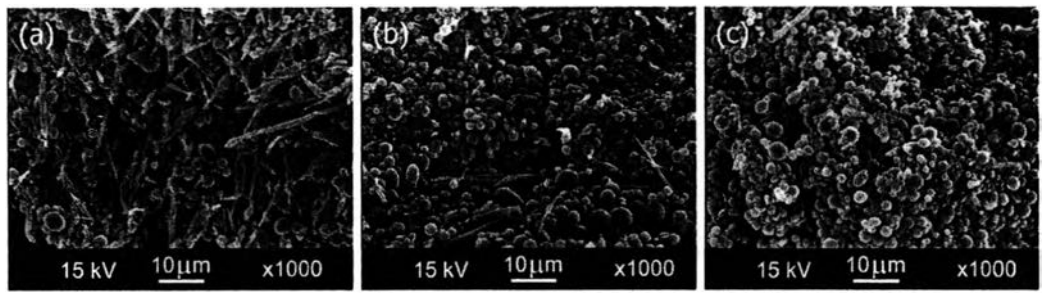

Figure 7.4 SEM images of the capillary rheometer extrudate after extrusion at 260°C, 1600 s^{-1} of (a) PVA, (b) PVA 0.5 ZnO, and (C) PVA 1 ZnO.

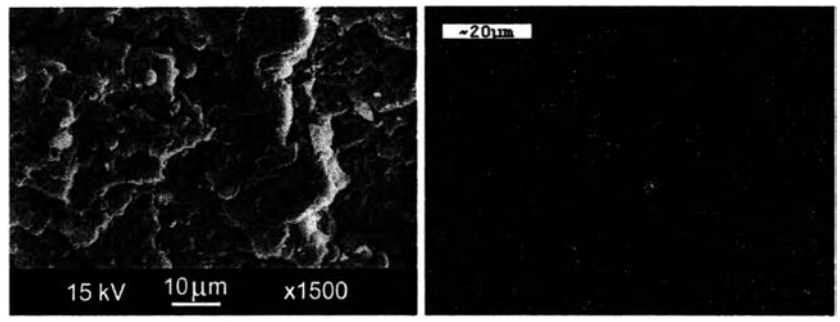

Figure 7.5 SEM (left) vs. EDX (right) images of the fractured surface of PVA 1 ZnO (Zn mapping).

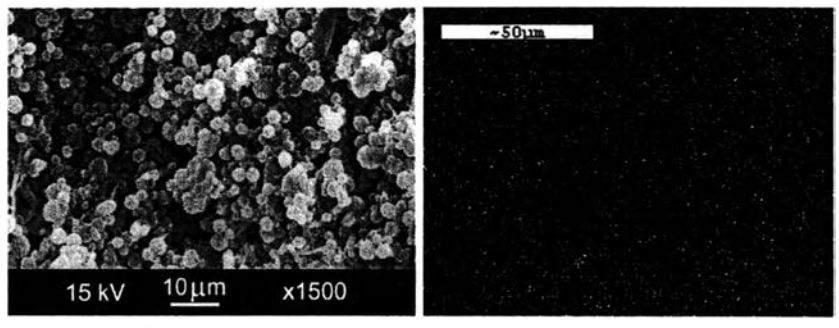

Figure 7.6 SEM (left) vs. EDX (right) images of the PVA 1 ZnO after dissolving the PET phase out (Zn mapping).

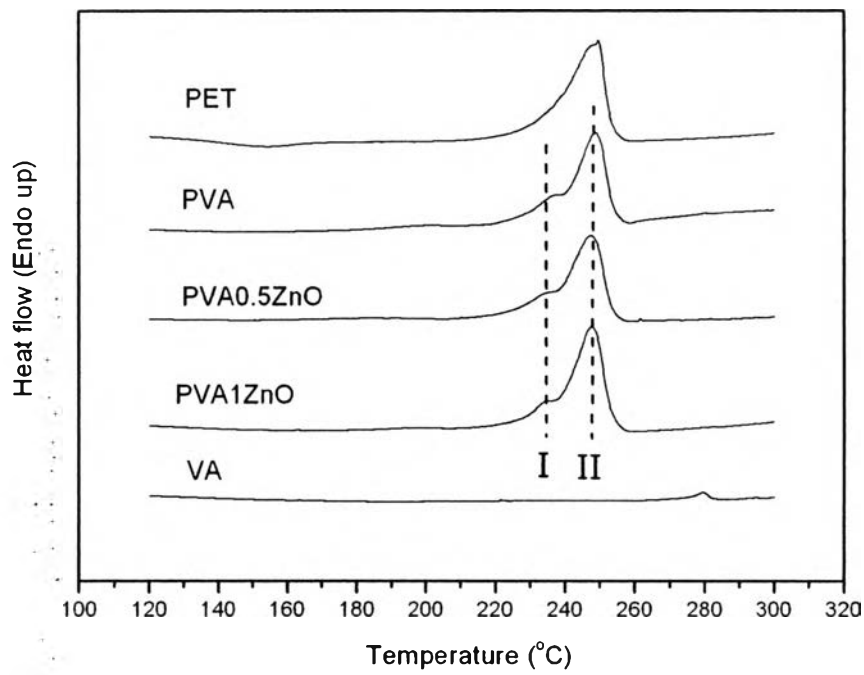

Figure 7.7 DSC heating scans (heating rate of 10°C/min).

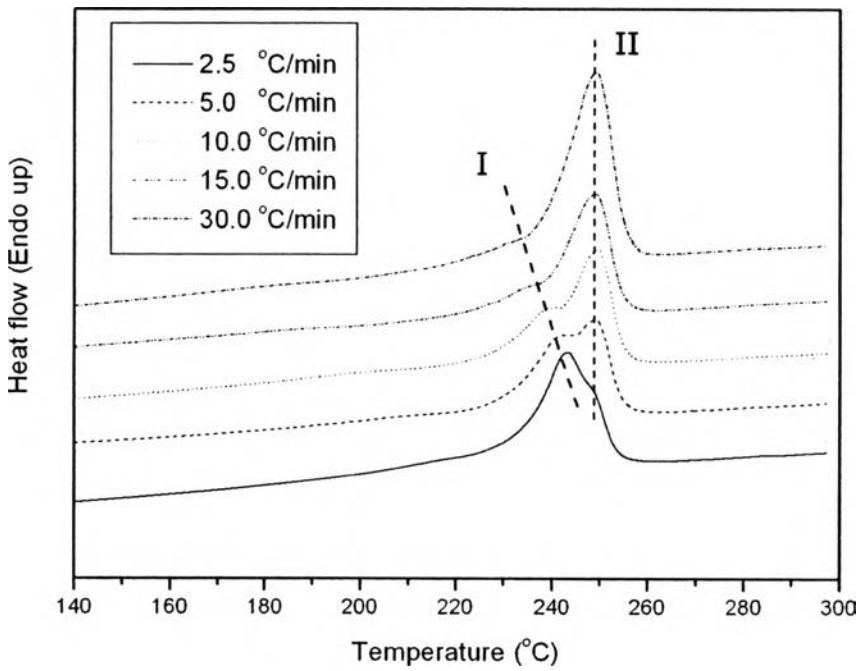

Figure 7.8 DSC heating scans performed at 10°C/min on the PET/VA samples after cooling at cooling rates ranging from 2.5 to 30°C/min.

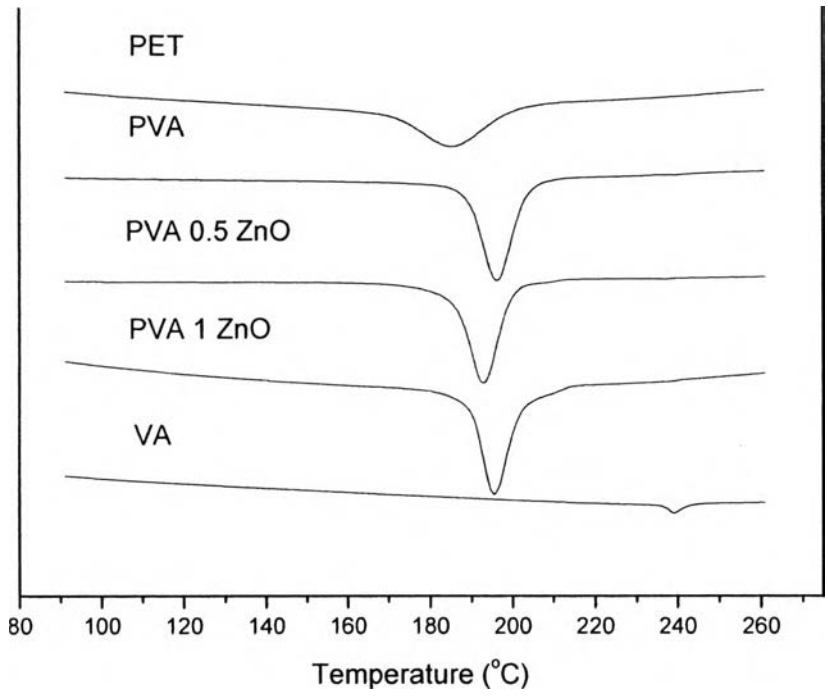

Figure 7.9 DSC cooling scans at a cooling rate of 10°C.

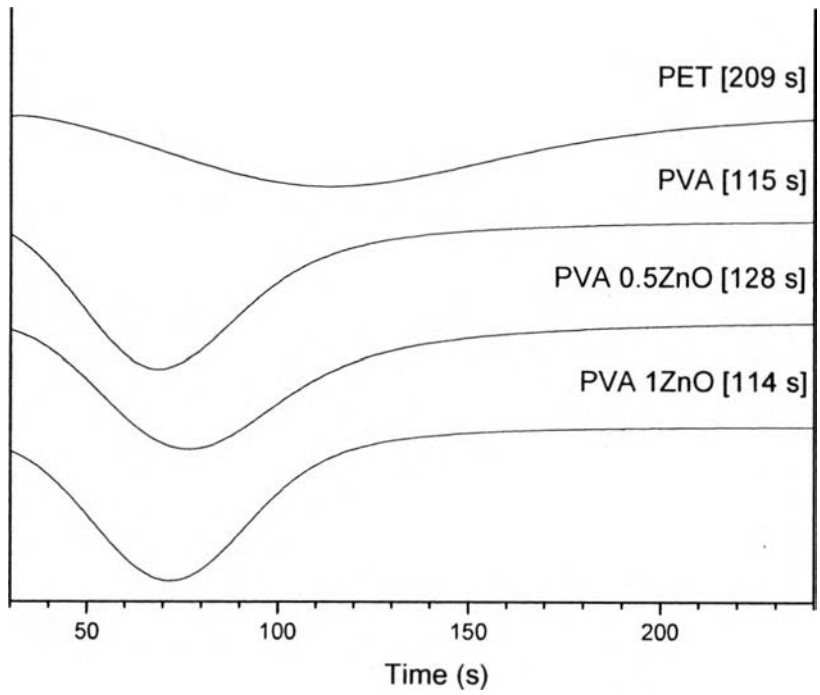

Figure 7.10 Isothermal melt crystallization at 200°C.

Table 7.1 Sample designations

Sample	PET (kg)	VA (kg)	ZnO (g)
PET	1	0	0
PVA (PET/10 wt% VA)	0.9	0.1	0
PVA 0.5 ZnO (PET/10 wt% VA/0.5 phr ZnO)	0.9	0.1	5
PVA 1 ZnO (PET/10 wt% VA/1.0 phr ZnO)	0.9	0.1	10

Table 7.2 Injection molding conditions for the neat PET, VA, and their blends

Sample	Temperature (°C)					
	Zone 1	Zone 2	Zone 3	Zone 4	Nozzle	Mold
PET	260	250	240	230	65	15
PVA	220	230	240	250	220	90
PVA 0.5 ZnO	235	245	255	265	220	90
PVA 1 ZnO	250	260	270	280	220	90

Table 7.3 Thermal characteristics of neat PET, PET/VA blends, and PET/VA/ZnO composites

Sample	Heating scans		Cooling scans			
	$T_{m,I}$	$T_{m,II}$	$T_{mc,on}$	$T_{mc,p}$	$T_{mc,end}$	ΔH_{mc}(-J/g)
PET	-	250.1	203.3	181.2	161.0	37.35
PVA	236.7	248.4	206.1	199.4	192.3	38.91
PVA 0.5ZnO	235.2	248.2	197.8	190.2	180.1	38.83
PVA 1ZnO	234.9	247.8	201.4	193.9	187.3	41.93

Table 7.4 Isothermal crystallization data of neat PET, PET/VA blends, and PET/VA/ZnO composites measured at 200°C

Sample	$t_{1/2}$(s)	Normalized ΔH_c (J/g)
PET	120	34.23
PVA	76	39.95
PVA 0.5ZnO	84	36.04
PVA 1ZnO	81	39.18

Table 7.5 The static mechanical properties of neat PET, PET/VA blends, and PET/VA/ZnO composites

Sample	Tensile Modulus (MPa)	Tensile Strength (MPa)	%elongation at break
PET	1144(9)	65.0(0.2)	398(75)
PVA	1329(16)	71.4(1.1)	7(1)
PVA 0.5ZnO	1354(47)	70.5(2.0)	6(1)
PVA 1ZnO	1471(47)	34.7(6.7)	3(1)

Note: Numbers in the parentheses represent the values of standard deviation.